Characterisation of interfacial adhesion in hemp composites after H2O2 and non-thermal plasma treatments

R Barbière, F Touchard, L Chocinski-Arnault, E Fourré, E Leroy, J Barrault

Characterisation of interfacial adhesion in hemp composites after H_2O_2 and non-thermal plasma treatments

R. Barbière[1], F. Touchard[1], L. Chocinski-Arnault[1], E. Fourré[2], E. Leroy[3], J. Barrault[3]

[1] *Département Physique et Mécanique des Matériaux, Institut Pprime*

CNRS-ENSMA-Université de Poitiers UPR 3346, ISAE-ENSMA

1 Avenue Clément Ader, 86961 Futuroscope cedex, France

[2] *Institut de chimie des Milieux et Matériaux de Poitiers*

IC2MP UMR CNRS 7285 Université de Poitiers

4 Rue Michel Brunet, Bât. B27

TSA 51106 - 86073 Poitiers cedex, France

[3] *Valagro Recherche*

4 Rue Marcel Doré, Bât. B14

86000 Poitiers, France

e-mail : romain.barbiere@ensma.fr

e-mail : fabienne.touchard@ensma.fr (corresponding author)

e-mail : laurence.chocinski@ensma.fr

e-mail : elodie.fourre@univ-poitiers.fr

e-mail : eleroy@valagro-rd.com

e-mail : joel2.barrault@gmail.com

Characterisation of interfacial adhesion in hemp composites after H_2O_2 and non-thermal plasma treatments

Abstract:

Interface optimisation for continuous hemp reinforcements in epoxy resin is a current challenge for the development of biocomposites. A chemical treatment based on hydrogen peroxide and a physical one using a non-thermal plasma have been tested to optimise interface adhesion, by varying several parameters. FTIR analysis and FE-SEM observations have shown the effects of the treatments on chemical and morphological aspects of the treated yarns. Tensile tests on hemp yarns have allowed the selection of the treatment parameters leading to the best strength. Fragmentation tests results showed that the two treatments lead to a decrease in the fragment lengths and thus, an enhancement of the Interfacial Shear Strength (IFSS) values in comparison with the untreated yarn. This is confirmed by the micro-CT observations of the debonding lengths in the vicinity of each yarn fragment extremity. Finally, the plasma treated samples exhibit a better interface adhesion quality (IFSS=44.7±4MPa) than the chemically treated ones (IFSS=24.2±4MPa), which are better than the non-treated ones (IFSS=13.5±4MPa).

Keywords: interfacial adhesion ; fragmentation tests ; hemp/epoxy composites ; hydrogen peroxide; plasma.

1. Introduction

The environmental consciousness as well as the European legislation has encouraged academic and industrial research to develop eco-friendly, sustainable and recyclable composite materials, often referred to as “green composites”. The interest in natural plant fibres as reinforcement in polymer matrix has grown quickly in the last decade. Industries as automotive, shipbuilding and construction have started the manufacturing of products using natural fibres [1–4]. However, these biocomposites are mainly used for secondary or tertiary structures, because of their poor mechanical

properties, which depend on the individual mechanical properties of the matrix and fibres as well as on the fibre/matrix interfacial bonding. Interfacial adhesion between the fibres and the matrix plays a fundamental role in the mechanical characteristics of the composite [5-7]. The factors affecting the interfacial bonding between the fibre and matrix are the mechanical interlocking, the molecular attractive forces, the electrostatic adhesion and the chemical bonds. However, the naturally hydrophilic plant fibres are not inherently compatible with polymers, which are comparatively more hydrophobic [8]. In addition to the pectin and waxy substances in plant fibre acting as a barrier to interlock with nonpolar polymer matrix, the presence of numerous hydroxyl groups hinders its operative reaction with the matrix [9]. Therefore, the modification of the surface characteristics of plant fibre is essential in order to formulate a composite with superior interfacial bonding and effective stress transfer throughout the interface [10]. Two types of methods can improve the fibre-matrix interface: chemical and physical ones. Among the chemical ones, the most common treatments are using liquid ammonia, permanganates, isocyanates or consist in silane coupling, esterification and graft copolymerization [11]. Commonly used physical methods are thermo-treatment, electric discharge, corona or plasma treatment. In particular, non-thermal plasma process allows surface modification without the use of chemicals, nor solvents. It is a fast, environmentally friendly, nontoxic and dry process [12]. For this method, an ionised gas is created by applying enough energy to reorganise the electronic structure of the species present in the gas phase. This kind of treatment can be useful to activate the fibre surface and enhance the interfacial adhesion, as it has been shown, for example, in flax/polyethylene composites [13].

A number of studies have been carried out on the effects of different fibre surface treatments on the properties of natural fibre composites [5, 14, 15]. In particular, concerning hemp composites, the effect of NaOH treatments [16,17], silane treatments [18] or alkalisation treatments [19,20] have been studied. Other treatments based on vanillin alcohol [21] or on the deposition of reactive monomers by plasma [22] have also been tested. Most of the studies concern short fibre or mat

composites [23]. However, in those composites, the fibre orientation is random and, consequently, mechanical properties are not as high as in continuous fibre composites. There is a lack of data concerning the interface optimisation for continuous hemp reinforcements.

In the present study, continuous hemp reinforcement in epoxy matrix is used. Hemp (*Cannabis sativa* L.) is one of the oldest crops and is now considered as one of the most eco-friendly industrial fibres [24]. The aim of this work is to enhance the interface adhesion quality in hemp/epoxy composites. For this purpose, two different types of treatments are applied to hemp yarns. The first one consists in a chemical treatment using hydrogen peroxide and the second treatment is physical, using a non-thermal plasma. For each of these treatments, different parameters are tested and the chemical and morphological effects on hemp yarns are analysed by FTIR (Fourier Transform Infrared) spectroscopy and FE-SEM (field-emission gun scanning electron microscopy). The untreated and treated hemp yarns are tested in tensile loading in order to compare their strengths. The aim is to find a good compromise between the effectiveness of the treatment and the preservation of the yarn mechanical properties. Fragmentation tests on single yarn hemp/epoxy composite specimens are performed and interfacial shear strength (IFSS) values are determined after measuring the obtained fragment lengths. It allows the characterization of the yarn/matrix interface adhesion quality at the relevant scale, without the influence of other neighbouring yarns. Moreover, this type of interface test not only allows to check the adhesion quality but also the mechanical properties of the chosen yarn-matrix couple [25]. A complete analysis of the interfacial debonding mechanism is also carried out using X-ray micro-CT.

2. Materials and methods

2.1 Tested materials

Hemp yarns were provided by Lin et L'autre (France). They were made of bundles of hemp fibres twisted together with a mean twisting angle around 11° and a linear density of about 83tex, as determined in a previous study [26]. The untreated hemp yarns were used as reference and noted

"Ref". The tested hemp yarns were considered cylindrical; their mean diameter was measured using an optical microscope and was found to be equal to 308±25µm.

The single yarn composite specimens were manufactured with resin injection moulding technique. The used resin is the EPOLAM 2020 epoxy resin from Axson. A special mold was developed to elaborate composite samples with a single hemp yarn aligned in the loading direction. The specimens were dogbone shaped, with a gauge section of 15mm long, 3mm wide and 2mm thick (Fig. 1). They were cured with the following cycle: 24h at ambient temperature, 3h at 40°C, 2h at 60°C, 2h at 80°C and 4h at 100°C, to achieve a cross-linkage as complete as possible. The final glass transition temperature measured by DSC (Differential Scanning Calorimetry) was 89 ± 2°C [27].

2.2 Hydrogen peroxide treatments

At first, hemp yarns were dried under vacuum at 60°C during 24h. Then they were immersed in a basic solution of hydrogen peroxide during 15 minutes at room temperature. Three different treatments with various concentrations of H_2O_2 (weight %) were used: 10%, 30% and 50%, noted H-T10, H-T30 and H-T50 respectively. Hemp yarns were then washed in distilled water and finally dried. Two different types of drying sequence were applied. For each treatment, hemp yarns were either dried under vacuum at 60°C during 24h, or dried in oven at 103°C during 24h. These two drying sequences were noted S1 and S2 respectively. Six different H_2O_2 treatments were thus obtained: H-T10S1, H-T10S2, H-T30S1, H-T30S2, H-T50S1 and H-T50S2.

2.3 Non-thermal plasma treatments

For the non-thermal plasma treatment, the reactor that was used had a cylindrical configuration (Fig. 2). The first electrode consisted in a stainless steel coiled filament, fitting to the inner wall of the glass cylinder (4cm diameter). The second electrode was a copper sheet (Advance tape) taped around the external wall of the cylinder. The total height of the plasma surface in the cylinder was

10cm. The electrodes were connected to a high voltage generator (A2E Technologies Enertronic) providing bipolar pulses. The signals were measured via two high voltage probes (Lecroy, PPE20KV-CC) and a current probe (Stangenes Industry 60MHz) connected to an oscilloscope (Lecroy WaveSurfer, 64Xs-A, 600MHz). Different parameters were tested for hemp yarn treatment, via the chemical nature of the gas (air or O_2; flow rate: 100ml.min^{-1}), the consumed energy (15 or 25W) and the duration of the treatment (2 to 10min). The yarns were placed around the filament coil and three different plasma treatments were compared: a treatment in air atmosphere with a power of 25W (noted Pl-T1), a treatment also in air atmosphere but with a power of 15W (noted Pl-T2) and a treatment in pure oxygen with a power of 25W (noted Pl-T3).

2.4 FTIR

Fourier Transform Infrared (FTIR) spectra of untreated and treated hemp yarns were recorded. For the chemical treatments, a Thermo 6700 FTIR spectrometer (resolution: 2cm^{-1}, 16 scans) equipped with a deuterated-triglycine sulfate (DTGS) detector was used. For the plasma treatments, a Perkin Elmer FTIR (Spectrum One) spectrometer was used, in the range of 4000-650cm^{-1}. The spectra were normalised for comparison. Each yarn was analysed at three different positions after each treatment in order to evaluate the homogeneity of the treatment.

2.5 Microscopy

A morphological investigation of the surface of treated and untreated hemp yarns was carried out using a field-emission gun scanning electron microscope (FE-SEM) JEOL JSM-7000F. All specimens were sputter coated with gold prior to FE-SEM observation. After fragmentation tests, the fragment lengths were measured by using a Leica MZ95 microscope.

2.6 Micro-CT

A micro-CT analysis was performed using an UltraTom CT scanner manufactured by RX Solution (France). The system consists in a Hamamatsu micro focus sealed X-ray tube operating at 20-150kV/0-500 µA, within a maximum power of 75W. X-rays, generated by the source, diverge at an

angle providing a cone-beam. Various geometric magnifications can thus be obtained by moving the sample close to the source to provide high resolution mode or close to the detector to provide low resolution measurements. The generator and the detector are also mobile to cover a large range of magnification. A 1.5µm resolution was used in this work, with an accelerating voltage of 65kV and a beam current of 144µA. The image acquisition time was about 6h per specimen. The 3D reconstruction was performed using an algorithm based on the filtered back-projection procedure for Feldkamp cone beam geometry.

2.7 Tensile testing

Tensile tests were performed on single hemp yarns according to ASTM C-1557. Each yarn was mounted on paper frames with a central window of 10mm long. Hemp yarns were tested using an INSTRON 1195 machine with a load cell of 500N and a crosshead speed of 0.1mm/min. At least ten tests were performed for each type of yarn.

2.8 Fragmentation tests

The investigation of the interfacial adhesion of hemp yarns in epoxy resin was achieved via fragmentation tests. When applying a tensile loading to single hemp yarn composites, the load is transferred through the matrix into the yarn by means of shear stress at the interface. Yarn failure occurs when this transferred stress reached the tensile strength of the yarn. The yarn will continue to fracture into shorter length fragments as the load increases, until the yarn fragments are so small that the tensile stresses induced in the yarn can no longer reach the yarn tensile strength. At this point, a state of saturation is reached and the fragmentation process ceases. The fragmentation tests were performed using the INSTRON 1195 machine with a load cell of 500N. Tests were carried out at a rather low loading rate (0.01mm/min) in order to reach the fragmentation saturation level before the specimen failure. The loading phase was stopped if the specimen failed, or when the fragmentation saturation level was achieved, which, in the present case, was defined as occurring when no new yarn break appeared during a subsequent strain increase by 0.5%, as frequently

reported in literature [28]. 80 grit sand papers were used in the jaws to improve clamping. After testing, fragment lengths were measured using an optical microscope and a statistical analysis was performed.

3. Results and discussion

3.1 Chemical and morphological effects on hemp yarns

Peroxide is a chemical compound with the functional group ROOR containing the divalent ion bond O-O. In contrast to oxide ions, the oxygen atoms in the peroxide ion have an oxidation state of -1. It is inclined to decompose to free radicals of the form RO•, and then the RO• can be grafted onto the cellulose macromolecule polymer chain by reacting with the hydrogen groups of plant fibre, as explained by Zhou et al. [5]. In order to investigate the effect of the hydrogen peroxide treatments on the chemical composition of hemp yarns, Fourier Transform Infrared (FTIR) analysis was performed. As examples, FTIR spectra in Fig. 3 show the results for the untreated (reference) hemp yarn and the hemp yarns after H-T10S2 (10%, 103°C) and H-T50S2 (50%, 103°C) treatments. Untreated hemp yarn consists of alkane, esters, aromatics, ketone and alcohol belonging to cellulose, hemicellulose and lignin [29]. Signals between 3600 and 3000cm^{-1} are consistent with stretching vibration of OH bonds of cellulose and hemicellulose (Table 1). Fig. 3 shows that this part of the spectrum reveals the presence of hydrogen bonding in the intra and inter molecular cellulose network. Similar effects can be observed over IR bands in the 2935-2862cm^{-1} domain (C-H bond stretching) and in the 1125-895cm^{-1} domain (which characterises the polysaccharidic nature of fibres). The hydrogen peroxide activation modified the infrared signals. Overall, a sharpening of the main infrared bands can be observed. It is due to the fact that the peroxide treatment led to the removal of lignin, waxy substances and impurities, the 50% H_2O_2 concentration being slighter more beneficial to oxidation than the 10% one. The main change is observed on the band at 1735cm^{-1}. This can be attributed to the formation of carbonyl and/or carboxylic bonds (from the oxidation

treatment). It is also worth mentioning that this band is more important for the H-T50S2 sample than for the H-T10S2 one. Similar results were obtained for the drying sequence S1.

FTIR results were confirmed by FE-SEM analysis, which revealed the surface morphology of the untreated (reference) and hydrogen peroxide treated hemp yarns. Fig. 4 allows the comparison of the three different H_2O_2 concentrations, 10%, 30% and 50%, for the drying sequence S2. The higher the H_2O_2 concentration, the cleaner the hemp fibres due to the leaching out of waxes, gums and pectic substances. The fibrillar structure of the yarn with the individual ultimate fibres is revealed for the strongest treatment H-T50S2, even if there is still some remaining external substances (Fig. 4c).

For the non-thermal plasma treatment, different durations were tested. For 2min duration, an inhomogeneous oxidation of the yarn surface was detected by FTIR analysis at different locations along the yarn. For 10min duration, a degradation of the yarn was observed, with a color change to dark brown. Finally, an intermediate treatment time of 5min was chosen and different gas flow chemical natures and power values were tested. FTIR spectra for Pl-T1 (air, 25W), Pl-T2 (air, 15W) and Pl-T3 (O_2, 25W) treatments are presented in Fig. 5. Oxidation is visible on every spectrum with the appearance of a band at 1735cm^{-1}, corresponding to a C=O stretching bond. In terms of band intensities, the strongest oxidation was obtained after 5min of air plasma at 15W (Fig. 5A) and O_2 plasma at 25W (Fig. 5C).. The band at 1635cm^{-1} corresponds to OH band from water (Table 1). FE-SEM observations on plasma treated hemp yarns showed no clear differences with the untreated yarn, demonstrating that there is no significant modification of the yarn surface morphology after this type of treatment.

3.2 Tensile strength of treated and untreated hemp yarns

The aim of chemical and physical treatments applied on hemp yarns is to enhance the interfacial adhesion between yarns and epoxy matrix. However, these treatments can also have consequences

on the yarn mechanical properties. A compromise has to be done between the treatment efficiency and the residual mechanical properties of the yarns. Indeed, the composite laminates made of treated yarns should have good interfacial adhesion quality together with high mechanical characteristics. Therefore, tensile tests were realised on single hemp yarns and a first selection between the different treatments was performed thanks to the comparison of the tensile strength values (σ_u) between treated and untreated yarns (Table 2). First results concern the chemically treated hemp yarns. As it can be seen in Fig. 6, despite the experimental dispersion, the global tendency shows that the drying sequence S2 (i.e. in oven at 103°C during 24h) leads to slightly higher mean values than the drying sequence S1 (i.e. under vacuum at 60°C during 24h). Moreover, all the treatments allow to obtain higher mean σ_u values than the one measured for untreated hemp yarns. The maximum σ_u value is reached for the H-T10S2, i.e. the treatment with the lowest H_2O_2 concentration level. Therefore, H-T10S2 samples were selected for the fragmentation tests.

The same analysis was performed on plasma treated hemp yarns. Fig. 7 shows the results obtained for the three different plasma tests. The plasma treatments with the highest power value (25W) lead to a decrease in the tensile strength of the hemp yarns, independently of the gas flow chemical nature. The hemp yarns with the plasma treatment Pl-T2 (air, 15W) are the only ones to exhibit a mean σ_u value equivalent to the one of the untreated hemp yarns. This treatment is also the most ecological one, using less energy and being under air atmosphere. Therefore, this plasma treatment has been selected for fragmentation tests.

3.3 Interfacial shear strength

Fragmentation tests were performed on single hemp yarn/epoxy samples for the three selected types of yarns: untreated ones (reference), H_2O_2 treated yarns (H-T10S2) and plasma treated yarns (Pl-T2). An example of fragmentation test is shown in Fig. 8. By looking carefully at the tensile curve, it is possible to observe a slight decrease in the stress at each fragmentation occurrence (Fig. 8b). At the end of the test, after the sample failure, several fragments are visible in the gauge length (Fig.

8c). Each fragment length, l_f, is then measured by optical microscopy on all the tested samples. The critical fragment length value can thus be determined by using Eq. 1 [31]:

$$l_c = \frac{4}{3} l_f \quad \text{Eq. 1}$$

It allows plotting the Weibull distribution of critical fragment lengths for each tested configuration (Fig. 9). Despite the dispersion, results show that the samples with the treated hemp yarns exhibit lower l_c values than the untreated ones. Moreover, samples with the plasma treatment show lower l_c values than samples with the H_2O_2 treatment (Fig. 9).

In order to compare the adhesion quality of the different treatments, the IFSS (Interfacial Shear Strength) values have been calculated using Eq. 2 based on the Kelly and Tyson law [25,32]:

$$IFSS = \frac{2 \times F_u^{l_c}}{\pi \times l_{cw} \times \Phi_a} \quad \text{Eq. 2}$$

where l_{cw} is the representative critical fragment length determined by Weibull analysis, $F_u^{l_c}$ is the yarn ultimate tensile force extrapolated at a length equal to the critical fragment length l_c and determined thanks to the Weibull parameters [33], and Φ_a the average hemp yarn diameter. Results are reported in Table 3. Results show that treatments lead to an increase in the IFSS values in comparison with the untreated material. The plasma treatment seems to be the most efficient with the greatest increase in the adhesion quality (44.7MPa vs 13.5MPa for the untreated sample). This high IFSS value is directly linked to the decrease in the fragment length of more than fifty percent compared to the untreated single yarn composite (Table 3).

After fragmentation tests, a morphological investigation of the fracture surface has been performed using the FE-SEM. Fig. 10 shows micrographs obtained on single yarn composites with untreated and treated hemp yarns. Two treatments are compared: the H_2O_2 treatment H-T10S2 (10%, 103°C) and the plasma treatment Pl-T2 (air, 15W). For the H_2O_2 treatment, it can be seen in Fig. 10a that many elementary hemp fibres have been pulled out from the matrix at the moment of failure in the reference sample. Fewer fibres have been pulled out from the matrix in the case of the treated hemp yarns (Fig. 10b and c), which confirms the better interfacial adhesion after the treatments.

Moreover, for the plasma treatment, Fig. 10c shows that many fibres are still well-bonded to the matrix and have broken in the matrix failure plane. It confirms the better adhesion quality obtained with the plasma treatment.

3.4 Interfacial debonding

Another parameter allowing the comparison of the interfacial adhesion quality is the debonding length, characterising the interfacial decohesion which occurs around each yarn failure. Fig. 11a presents a micrograph, acquired with polarised light, of a single untreated hemp yarn/epoxy composite after fragmentation test and before sample failure. As it can be seen in Fig. 11b, the debonding length values, l_d, can be easily measured as the length of the black area around each yarn failure. Therefore, the debonding length values were determined by optical micrography observations around each fragmentation in the tested samples for the three configurations: with untreated yarns (reference), with Pl-T2 (Plasma, air 15W) treated yarns and with H-T10S2 (H_2O_2, 10% 103°C) ones. The obtained Weibull distributions are plotted in Fig. 12. Results in Fig. 12 prove that the debonding lengths present the same ranking as for the critical fragment lengths in Fig. 9. For the two selected treatments, the debonding phenomenon is lower than for the untreated case. The lowest values are obtained for the single yarn composite samples made with plasma treated hemp yarns. Representative values of debonding lengths obtained by Weibull analysis for each configuration are given in Table 3.

Micro-CT observations were also performed on fragmented samples for each type of treatment. An example is given in Fig. 11 for an untreated sample. Thanks to the very fine micro-CT resolution (1.5µm for 1 voxel), it was possible to visualise the small black lines corresponding with the interfacial debonding between the hemp yarn and the matrix (Fig. 11c). By looking closely at the yarn cross-section in the sample, it appears that the yarn/matrix interface in the healthy zone of the gauge length (i.e. far from the yarn failure) is undamaged (Fig. 11e), while damage is present all around the yarn in the debonding zone near the yarn fragment extremity (Fig. 11d). By using the

micro-CT scans, it is also possible to build a 3D reconstruction of the damage near the yarn failure zone (Fig. 11f). It allows a real representation of the debonding phenomenon occurring at the yarn/matrix interface in such a composite material.

In Fig. 13, observations made by micro-CT in the (x,y) plane are presented for untreated yarn, H-T10S2 and Pl-T2 treated yarns. Focus is done on a yarn failure zone, allowing the measurement of the corresponding debonding length. These micro-CT observations show that the same average values of the interfacial debonding zone is obtained by the two methods, X-ray micro-CT and optical micrography, and the same classification can be made: the debonding phenomenon is more significant for the untreated hemp yarn than for the H_2O_2 treated one, which is more pronounced than for the plasma treated yarn. These results confirm that IFSS values determined by fragmentation tests on single yarn composites are directly linked with debonding lengths at the yarn/matrix interface. The higher the IFSS value, the shorter the interfacial debonding and thus, the better the adhesion quality at the interface. Therefore, the comparison between untreated and treated hemp/epoxy composites shows that hydrogen peroxide and non-thermal plasma treatments enhance the interfacial adhesion quality, the plasma method being more efficient than the chemical one. As the plasma method is the most “ecological” one, without chemicals nor solvents, these are promising results for the optimization of plant fibre composites.

4. Conclusion

The use of plant fibre composites for engineering applications has considerably increased in the recent years, especially for the transportation domain. Understanding the interface and bonding mechanisms of these composites is a key issue to maximise their industrial applications. This paper deals with the interface optimisation of continuous hemp reinforcements in epoxy resin using two different types of treatment. The first one consists in a chemical treatment based on hydrogen peroxide and the second one is a physical treatment using a non-thermal plasma. For these two methods, different parameters were studied: the H_2O_2 concentration and the drying sequence for the

hydrogen peroxide treatment; the duration, the chemical nature of the gas phase and the consumed energy for the plasma treatment. FTIR analysis and FE-SEM observations have shown the effects of both treatments on chemical and morphological aspects of the hemp yarns. Tensile tests on hemp yarns with and without treatments have allowed the selection of the parameters leading to the best tensile strength values. Single hemp yarn composite samples were then made with epoxy resin using an original specific mould, allowing to align the yarn in the longitudinal axis direction. Fragmentation tests were performed with three types of yarns: non-treated hemp yarns, chemically treated ones with a weight concentration of H_2O_2 of 10% and a drying sequence in oven at 103°C during 24h, and plasma (15W) treated yarn in air atmosphere during 5min. Results show that the two treatments lead to a decrease in the fragment lengths, thus enhancing the Interfacial Shear Strength (IFSS) values in comparison with the untreated yarn, the plasma treatment being the most effective. This was confirmed by micro-CT observations. Debonding lengths values measured around each fragmentation in the reference samples are higher than those measured in the H_2O_2 treated samples, which are themselves higher than those measured in the plasma treated ones.
The next step will be to apply these treatments at the fabric scale, in order to manufacture woven hemp/epoxy composites with treated reinforcement. If this up-scale step is quite easy for the H_2O_2 treatment, it has still to be developed for the non-thermal plasma one.

Acknowledgements:

This work was partially funded by the French Government program “Investissements d'Avenir” (EQUIPEX GAP, reference ANR-11-EQPX-0018) and by the CPER FEDER project of Région Nouvelle Aquitaine. It pertains to the French Government program “Investissements d’Avenir” (EUR INTREE, reference ANR-18-EURE-0010).

References:

1. Yashas Gowda TG, Sanjay MR, Subrahmanya Bhat K, et al. Polymer matrix-natural fiber composites: An overview. *Cogent Engineering*. 2018; 5. https://doi.org/10.1080/23311916.2018.1446667.

2. Thyavihalli Girijappa YG, Mavinkere Rangappa S, Parameswaranpillai J, et al. Natural Fibers as Sustainable and Renewable Resource for Development of Eco-Friendly Composites: A Comprehensive Review. *Front Mater*. 2019; 6: 226. https://doi.org/10.3389/fmats.2019.00226.

3. Gholampour A, Ozbakkaloglu T. A review of natural fiber composites: properties, modification and processing techniques, characterization, applications. *J Mater Sci*. 2020; 55: 829–92. https://doi.org/10.1007/s10853-019-03990-y.

4. Ramesh M. Flax (Linum usitatissimum L.) fibre reinforced polymer composite materials: A review on preparation, properties and prospects. *Progress in Materials Science*. 2019; 102: 109–66. https://doi.org/10.1016/j.pmatsci.2018.12.004.

5. Zhou Y, Fan M, Chen L. Interface and bonding mechanisms of plant fibre composites: An overview. *Composites Part B: Engineering*. 2016; 101: 31–45. https://doi.org/10.1016/j.compositesb.2016.06.055.

6. Latif R, Wakeel S, Zaman Khan N, et al. Surface treatments of plant fibers and their effects on mechanical properties of fiber-reinforced composites: A review. *Journal of Reinforced Plastics and Composites*. 2019; 38 :15–30. https://doi.org/10.1177/0731684418802022.

7. Perrier A, Touchard F, Chocinski-Arnault L, et al. Mechanical behaviour analysis of the interface in single hemp yarn composites: DIC measurements and FEM calculations. *Polymer Testing*. 2016; 52: 1-8, https://doi.org/10.1016/j.polymertesting.2016.03.019.

8. Perrier A, Touchard F, Chocinski-Arnault L, et al. Influence of water on damage and mechanical behaviour of single hemp yarn composites. *Polymer Testing*. 2017; 57: 17-25, https://doi.org/10.1016/j.polymertesting.2016.10.035.

9. Mohit H, Arul Mozhi Selvan V. A comprehensive review on surface modification, structure interface and bonding mechanism of plant cellulose fiber reinforced polymer based composites. *Composite Interfaces*. 2018; 25: 629–67. https://doi.org/10.1080/09276440.2018.1444832.

10. Bartos A, Anggono J, Farkas AE et al. Alkali treatment of lignocellulosic fibers extracted from sugarcane bagasse: Composition, structure, properties. *Polymer Testing*. 2020; 88-106549, https://doi.org/10.1016/j.polymertesting.2020.106549.

11. Kabir MM, Wang H, Lau KT, et al. Chemical treatments on plant-based natural fibre reinforced polymer composites: An overview. *Composites Part B: Engineering*. 2012; 43: 2883–92. https://doi.org/10.1016/j.compositesb.2012.04.053.

12. Ventura H, Claramunt J, Rodríguez-Pérez MA, et al. Effects of hydrothermal aging on the water uptake and tensile properties of PHB/flax fabric biocomposites. *Polymer Degradation and Stability*. 2017; 142: 129–38. https://doi.org/10.1016/j.polymdegradstab.2017.06.003.

13. Enciso B, Abenojar J, Paz E, et al. Influence of Low Pressure Plasma Treatment on the Durability of Thermoplastic Composites LDPE-flax/coconut under Thermal and Humidity Conditions. *Fibers and Polymers*. 2018; 19: 1327–34. https://doi.org/10.1007/s12221-018-1086-4.

14. Werchefani M, Lacoste C, Belguith, H, et al. Effect of chemical and enzymatic treatments of alfa fibers on polylactic acid bio-composites properties. *J. of Composite Materials.* 2020; 54(30): 4959-4967. DOI: 10.1177/0021998320941579.

15. Tita SPS, Medeiros R, Tarpani JR, et al. Chemical modification of sugarcane bagasse and sisal fibers using hydroxymethylated lignin: Influence on impact strength and water absorption of phenolic composites. *J. of Composite Materials*. 2018; 52(20): 2743-2753. DOI: 10.1177/0021998317753886.

16. Le Troëdec M, Rachini A, Peyratout C, et al. Influence of chemical treatments on adhesion properties of hemp fibres. *Journal of Colloid and Interface Science*. 2011; 356(1): 303-310, https://doi.org/10.1016/j.jcis.2010.12.066.

17. George M, Mussone PG, Abboud Z, et al. Characterization of chemically and enzymatically treated hemp fibres using atomic force microscopy and spectroscopy. *Applied Surface Science*. 2014; 314: 1019-1025, https://doi.org/10.1016/j.apsusc.2014.06.080.

18. Moonart U, Utara S. Effect of surface treatments and filler loading on the properties of hemp fiber/natural rubber composites. *Cellulose*. 2019; 26: 7271–7295, https://doi.org/10.1007/s10570-019-02611-w.

19. Mazzanti V, Pariante R, Bonanno A, et al. Reinforcing mechanisms of natural fibers in green composites: Role of fibers morphology in a PLA/hemp model system. *Composites Science and Technology*. 2019; 180: 51-59, https://doi.org/10.1016/j.compscitech.2019.05.015.

20. Dayo AQ, Zegaoui A, Nizamani AA, et al. The influence of different chemical treatments on the hemp fiber/polybenzoxazine based green composites: Mechanical, thermal and water absorption properties. *Materials Chemistry and Physics*. 2018; 217: 270-277, https://doi.org/10.1016/j.matchemphys.2018.06.040.

21. Touchaleaume F, Tessier T, Auvergne R, et al. Polyhydroxybutyrate/hemp biocomposite: tuning performances by process and compatibilisation. *Green Materials*. 2019; 7(4): 194-204, https://doi.org/10.1680/jgrma.19.00005.

22. Brunengo E, Conzatti L, Utzeri R, et al. Chemical modification of hemp fibres by plasma treatment for eco-composites based on biodegradable polyester. *Journal of Materials Science*. 2019; 54(23): 14367-14377, DOI: 10.1007/s10853-019-03932-8.

23. Tanasa F, Zanoaga M, Teaca CA, et al. Modified hemp fibers intended for fiber-reinforced polymer composites used in structural applications-A review. I. Methods of modification. *Polymer Composites*. 2020; 41(1): 5-31, DOI: 10.1002/pc.25354.

24. Manaia JP, Manaia AT, Rodriges L. Industrial Hemp Fibers: An Overview. *Fibers*. 2019; 7(12): 106. DOI: 10.3390/fib7120106

25. Seghini MC, Touchard F, Sarasini F, et al. Interfacial adhesion assessment in flax/epoxy and in flax/vinylester composites by single yarn fragmentation test: Correlation with micro-CT analysis. *Composites Part A: Applied Science and Manufacturing*. 2018; 113: 66–75. https://doi.org/10.1016/j.compositesa.2018.07.015.

26. Guillebaud-Bonnafous C, Vasconcellos D, Touchard F, et al. Experimental and numerical investigation of the interface between epoxy matrix and hemp yarn. *Composites Part A: Applied Science and Manufacturing*. 2012; 43: 2046–58. https://doi.org/10.1016/j.compositesa.2012.07.015.

27. Barbière R. Fatigue behaviour and interfacial optimization of a woven hemp/epoxy composite: moisture effect. PhD Thesis, ENSMA, Poitiers (France), 2020.

28. Joffe R, Andersons J, Wallström L. Interfacial shear strength of flax fiber/thermoset polymers estimated by fiber fragmentation tests. *J. Mater. Sci.* 2005; 40(9–10): 2721–2722. https://doi.org/10.1007/s10853-005-2115-4

29. Seghini MC, Touchard F, Sarasini F, et al. Effects of oxygen and tetravinylsilane plasma treatments on mechanical and interfacial properties of flax yarns in thermoset matrix composites. *Cellulose*. 2019. https://doi.org/10.1007/s10570-019-02785-3.

30. Célino A, Gonçalves O, Jacquemin F, et al. Qualitative and quantitative assessment of water sorption in natural fibres using ATR-FTIR spectroscopy. *Carbohydrate Polymers*. 2014; 101: 163–70. https://doi.org/10.1016/j.carbpol.2013.09.023.

31. Ohsawa T, Nakayama A, Miwa M, et al. Temperature dependence of critical fiber length for glass fiber-reinforced thermosetting resins. *J Appl Polym Sci*. 1978; 22: 3203–12. https://doi.org/10.1002/app.1978.070221115.

32. Kelly A, Tyson WR. Tensile properties of fibre-reinforced metals: Copper/tungsten and copper/molybdenum. *Journal of the Mechanics and Physics of Solids*. 1965; 13: 329–50. https://doi.org/10.1016/0022-5096(65)90035-9.

33. Zafeiropoulos NE. On the use of single fibre composites testing to characterise the interface in natural fibre composites. *Composite Interfaces*. 2007; 14: 807–20. https://doi.org/10.1163/156855407782106438.

Table 1: Main infrared vibration bands of plant fibres (from [30]).

Wave number (cm^{-1})	**Attribution**
3600-3000	Hydrogen bonded of OH stretching in cellulose and/or hemicelluloses
2935	CH stretching of cellulose and hemicelluloses
2862	CH_2 stretching of cellulose and hemicelluloses
1735	C=O stretching vibration of carboxylic acid in pectin or ester group in hemicelluloses
1635	OH bending vibration characteristic of sorbed water
1595	Aromatic ring in lignin
1502	Aromatic ring in lignin
1425	Carboxylic acid of pectin and COO^- vibration
1375	CH bending of cellulose and hemicelluloses
1335-1315	CH_2 wagging of cellulose and hemicelluloses
1275	Characteristic peak of lignin
1240	C-O of acetyl in pectin or hemicelluloses
1160	anti-symmetrical deformation of the C-O-C band
1125-895	C-O stretching and ring vibrational modes
895	Characteristic of β-links in cellulose
700-650	O-H out of plane bending

Table 2: Experimental tensile strength values of single hemp yarns for untreated (reference), hydrogen peroxide treated and plasma treated yarns.

Hemp yarn		σ_u (MPa)	Dispersion (MPa)
Untreated	Reference	219	53
Hydrogen peroxide treated	H-T10S1	246	44
	H-T10S2	287	47
	H-T30S1	235	50
	H-T30S2	278	42
	H-T50S1	255	52
	H-T50S2	267	43
Plasma treated	Pl-T1	191	54
	Pl-T2	217	48
	Pl-T3	187	51

Table 3: Yarn ultimate tensile force, representative critical fragment length, IFSS value and representative debonding length for untreated and treated hemp yarn/epoxy samples.

Hemp yarn treatment	$F_u^{l_c}$ (N)	l_{cw} (mm)	IFSS (MPa)	l_{dw} (mm)
Untreated (reference)	18.4 ± 3.5	3.2 ± 0.70	13.5 ± 4	0.46 ± 0.07
H-T10S2	27.5 ± 3.5	2.35 ± 0.15	24.2 ± 4	0.37 ± 0.04
Pl-T2	23.7 ± 3.5	1.4 ± 0.15	44.7 ± 4	0.30 ± 0.05

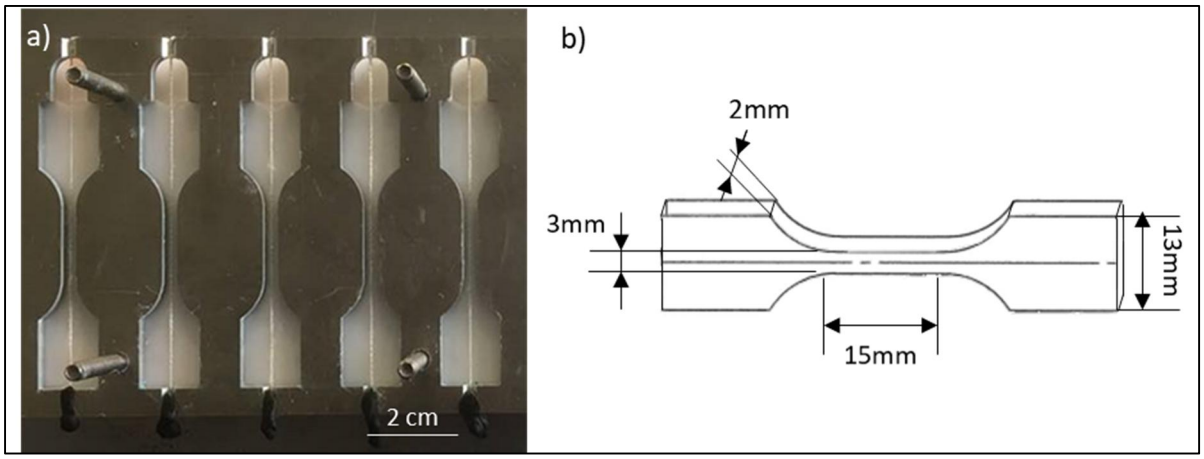

Fig. 1. a) Mould used for sample manufacture. b) Specimen geometry for the single yarn fragmentation tests.

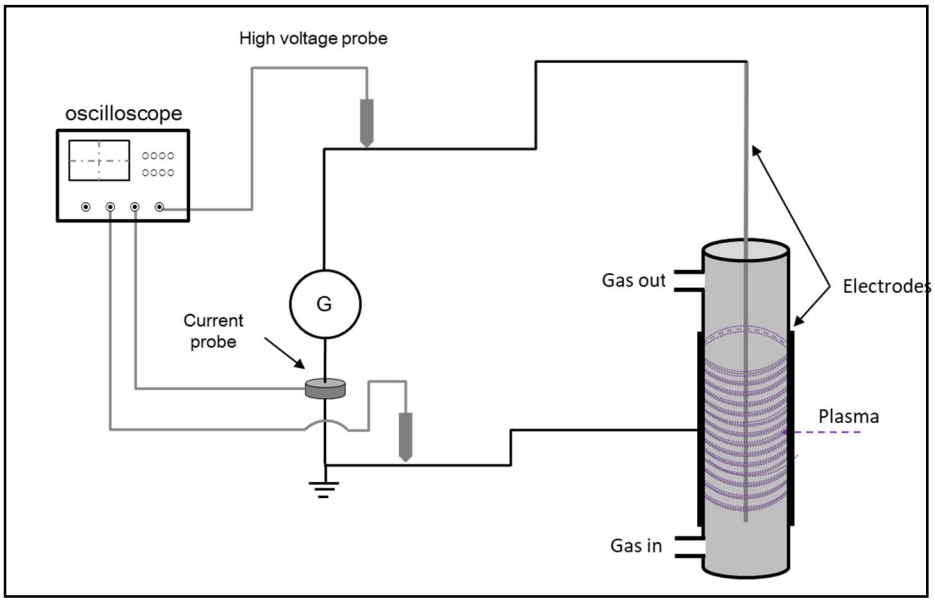

Fig. 2. Scheme of the non-thermal plasma reactor.

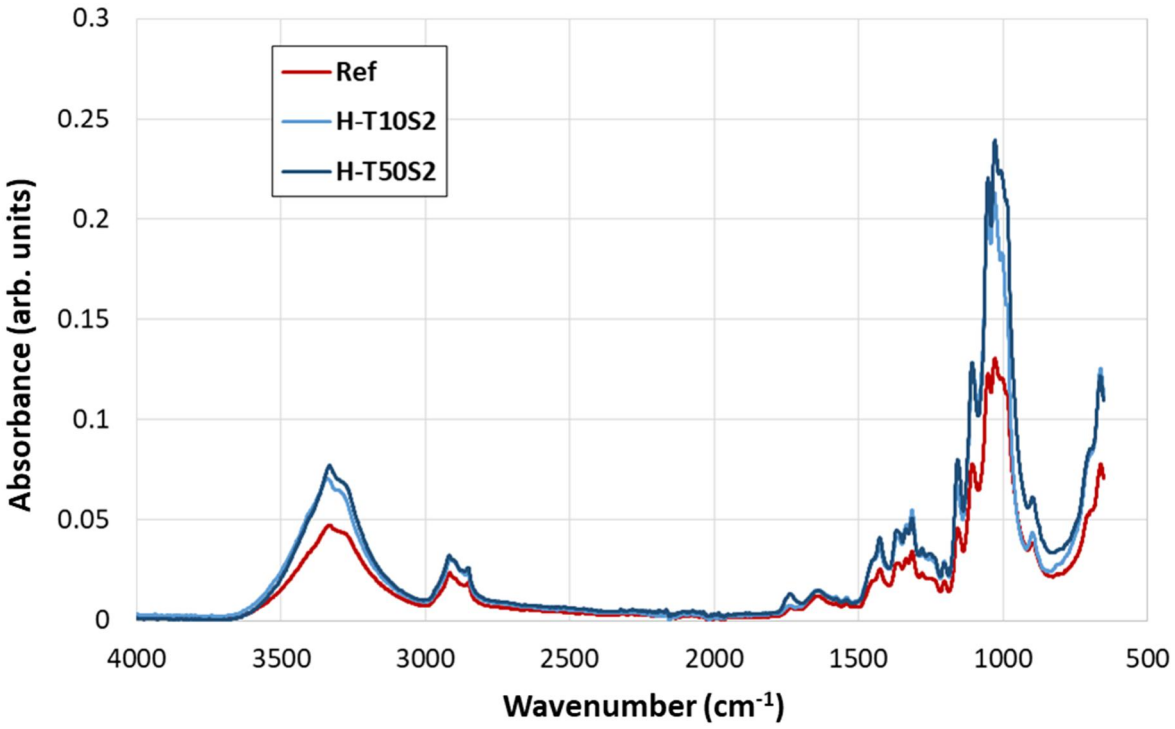

Fig. 3. Infrared spectra of the different hemp yarns: untreated (reference) and hydrogen peroxide treated (H-T10S2 and H-T50S2).

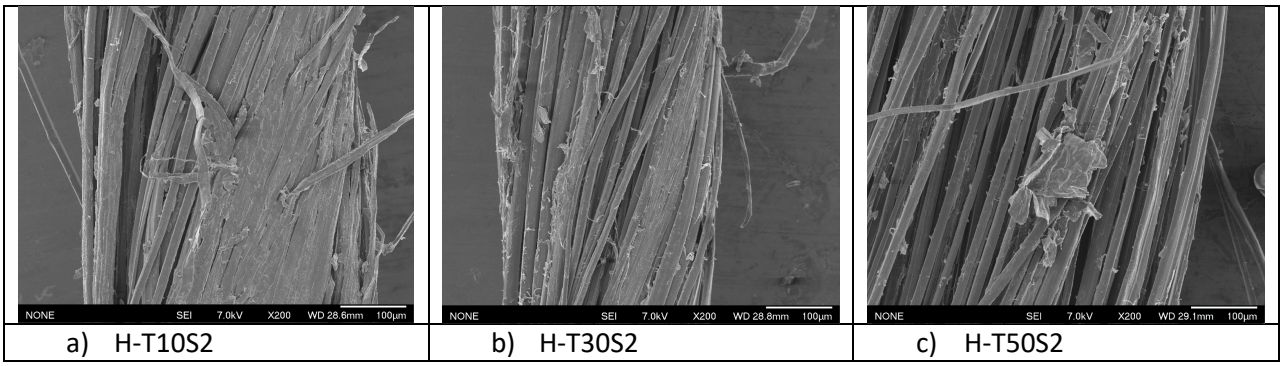

a) H-T10S2 | b) H-T30S2 | c) H-T50S2

Fig. 4. SEM micrographs of hydrogen peroxide treated hemp yarns for three different H_2O_2 concentrations: a) 10%, b) 30% and c) 50%, for the drying sequence S2.

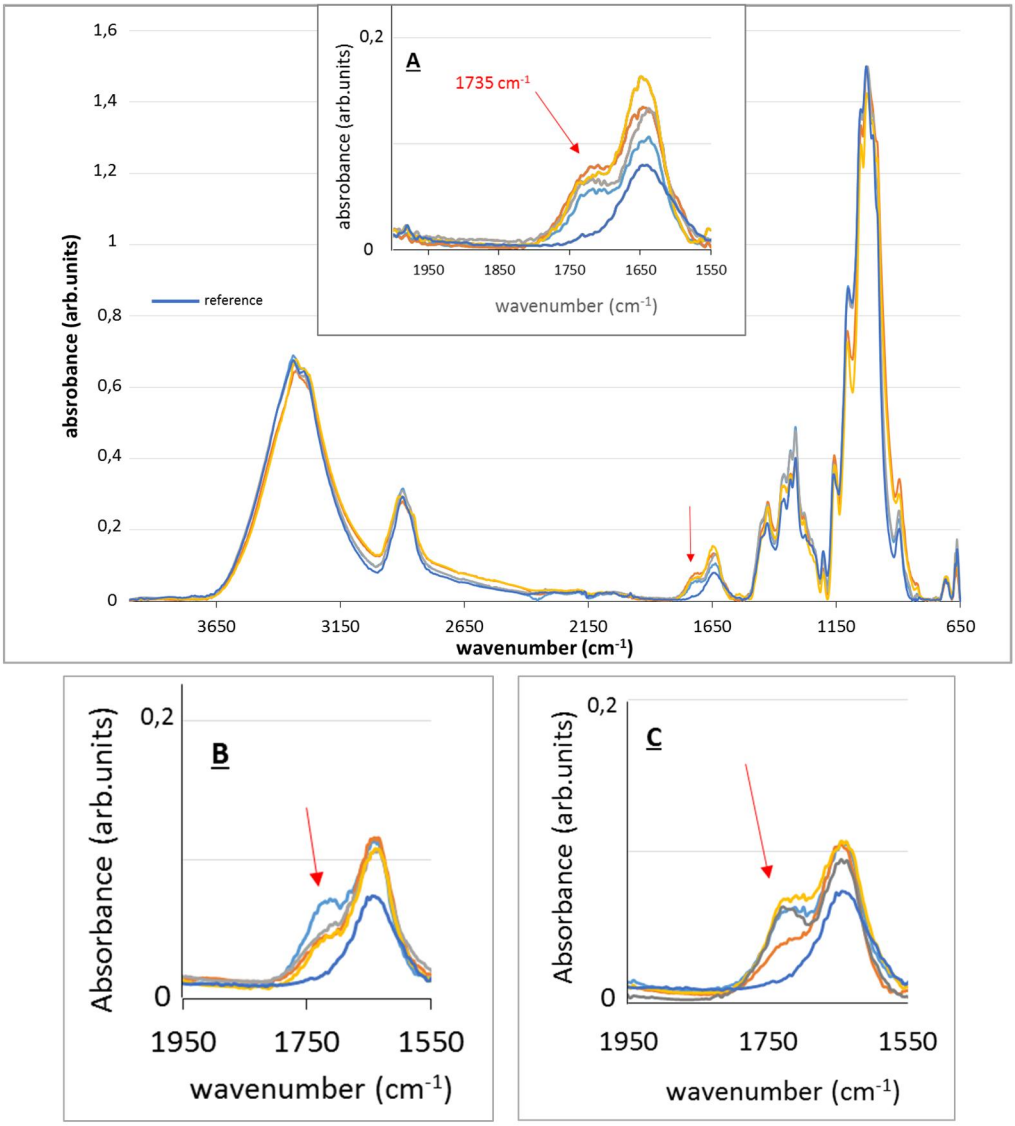

Fig. 5. Infrared spectra after 5 minutes of plasma treatment: A) Pl-T2: air, 15W; B) Pl-T1: air, 25W; C) Pl-T3: O_2, 25W. In each graph, the dark blue spectrum corresponds to the untreated hemp yarn (reference). The other color spectra were taken at four different locations on each treated hemp yarn.

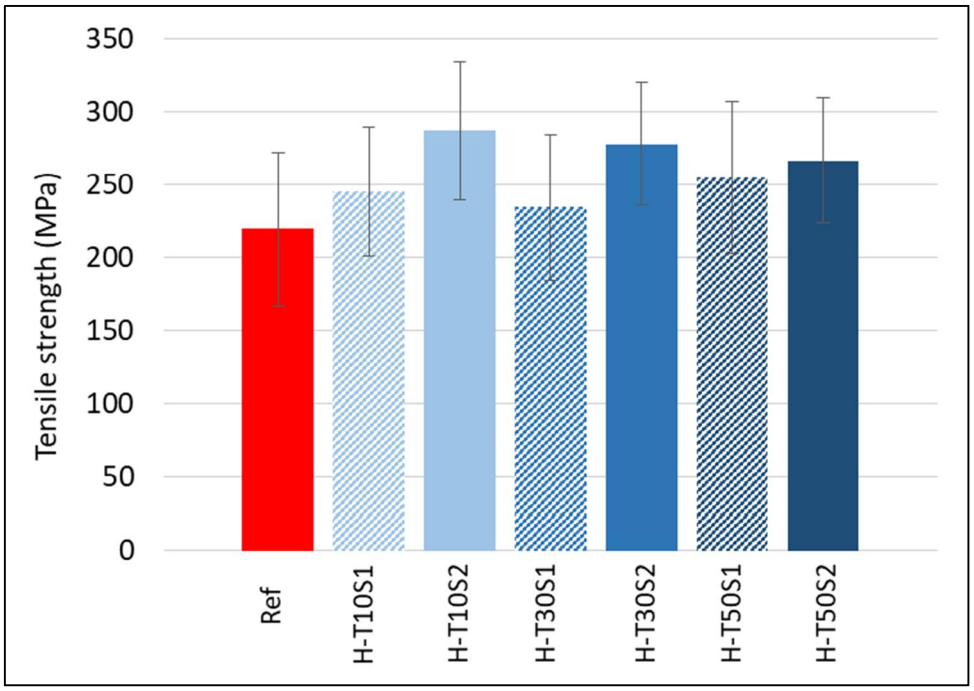

Fig. 6. Tensile strength values of untreated (reference) and hydrogen peroxide treated hemp yarns, for the three H_2O_2 concentrations and the two drying sequences.

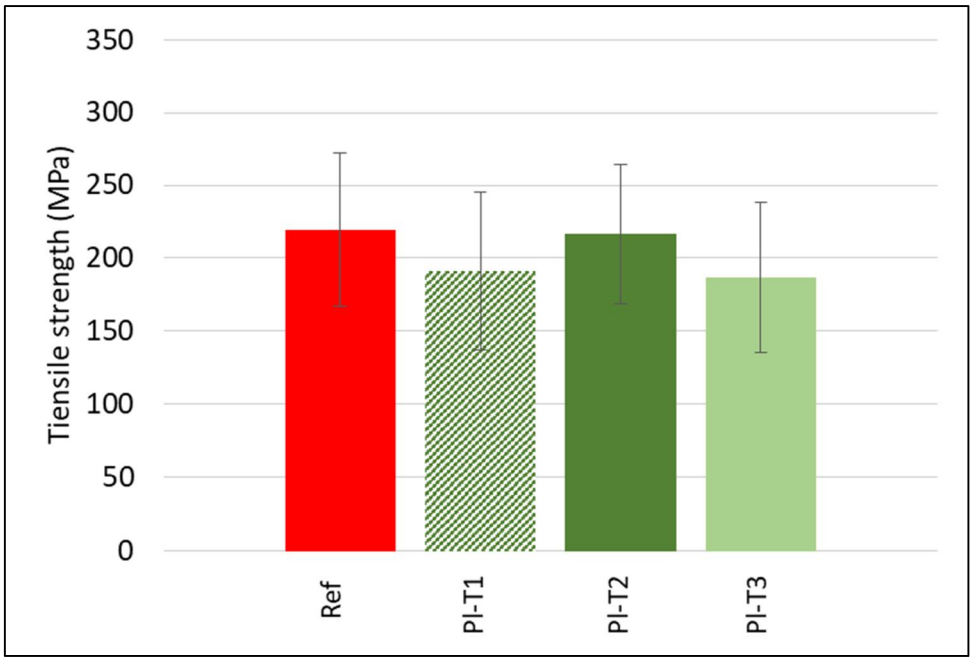

Fig. 7. Tensile strength values of untreated (reference) and plasma treated hemp yarns, for the three different configurations: Pl-T1 (air, 25W), Pl-T2 (air, 15W) and Pl-T3 (O_2, 25W).

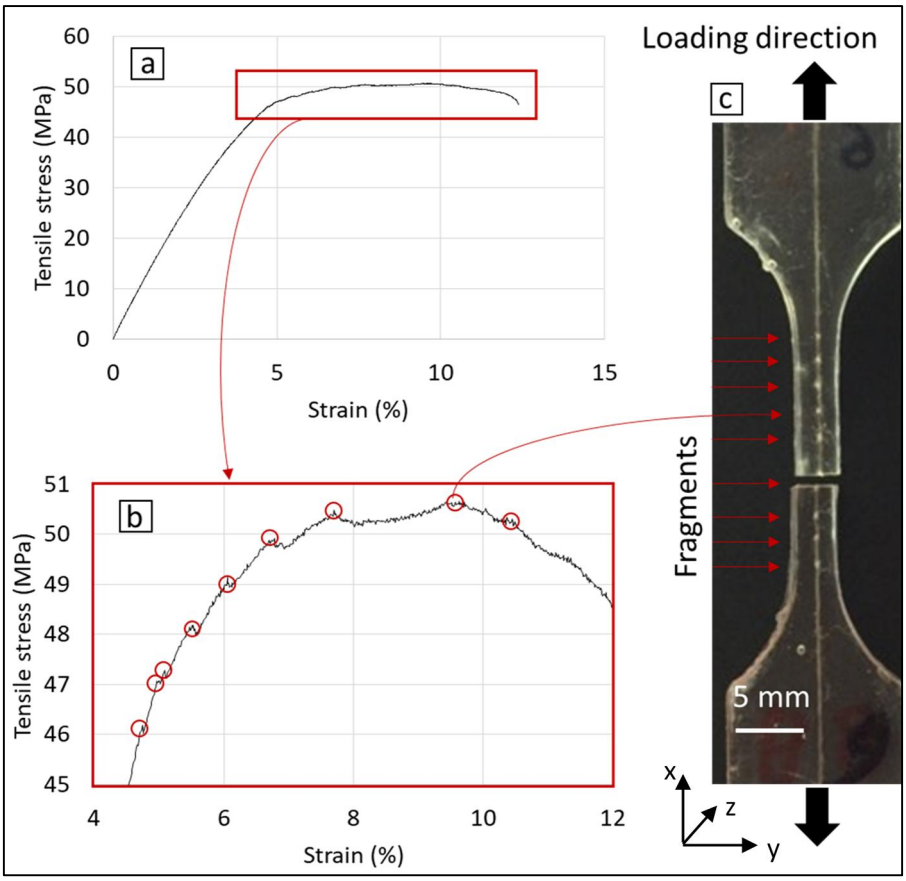

Fig. 8. Example of fragmentation test on a single hemp yarn/epoxy composite. a) full tensile curve, b) zoom on the tensile curve, c) hemp/epoxy sample with corresponding fragments.

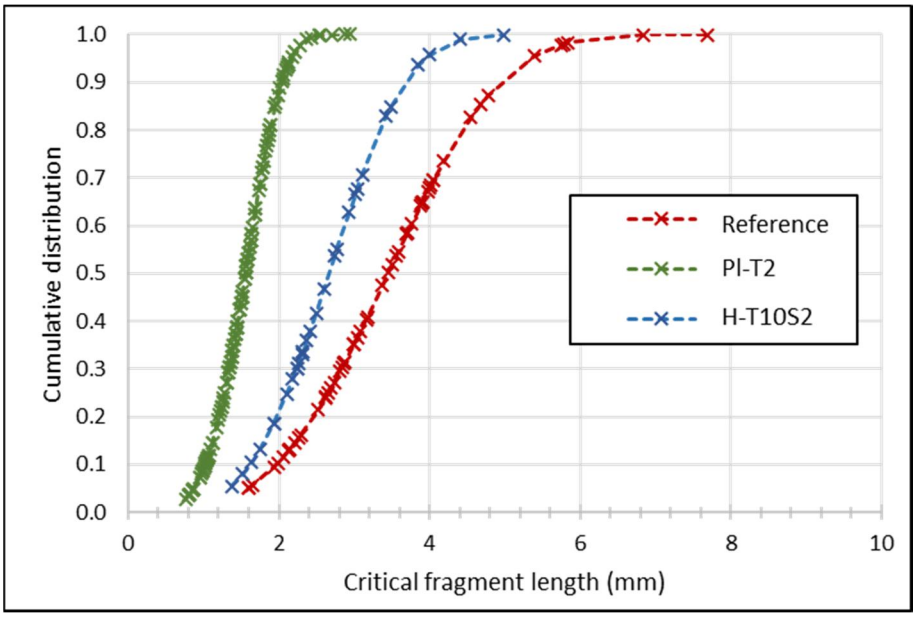

Fig. 9. Cumulative distribution of critical fragment lengths measured on single hemp yarn/epoxy composites for untreated (reference) and treated hemp yarns: Pl-T2 (Plasma, air 15W) and H-T10S2 (H_2O_2, 10% 103°C).

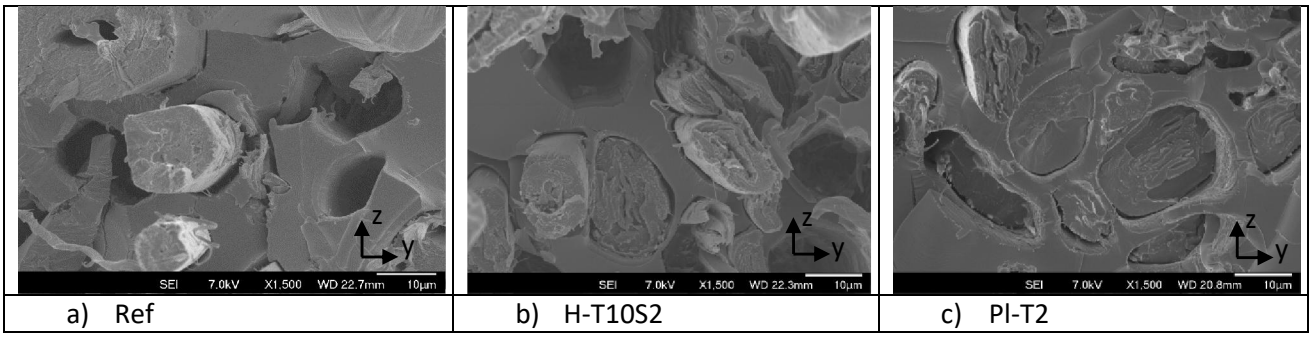

a) Ref	b) H-T10S2	c) Pl-T2

Fig. 10. SEM micrographs of single yarn composite fracture surfaces after fragmentation test. a) for untreated hemp yarn, b) for H_2O_2 treated hemp yarn H-T10S2 (H_2O_2, 10% 103°C) and c) for plasma treated hemp yarn Pl-T2 (Plasma, air 15W).

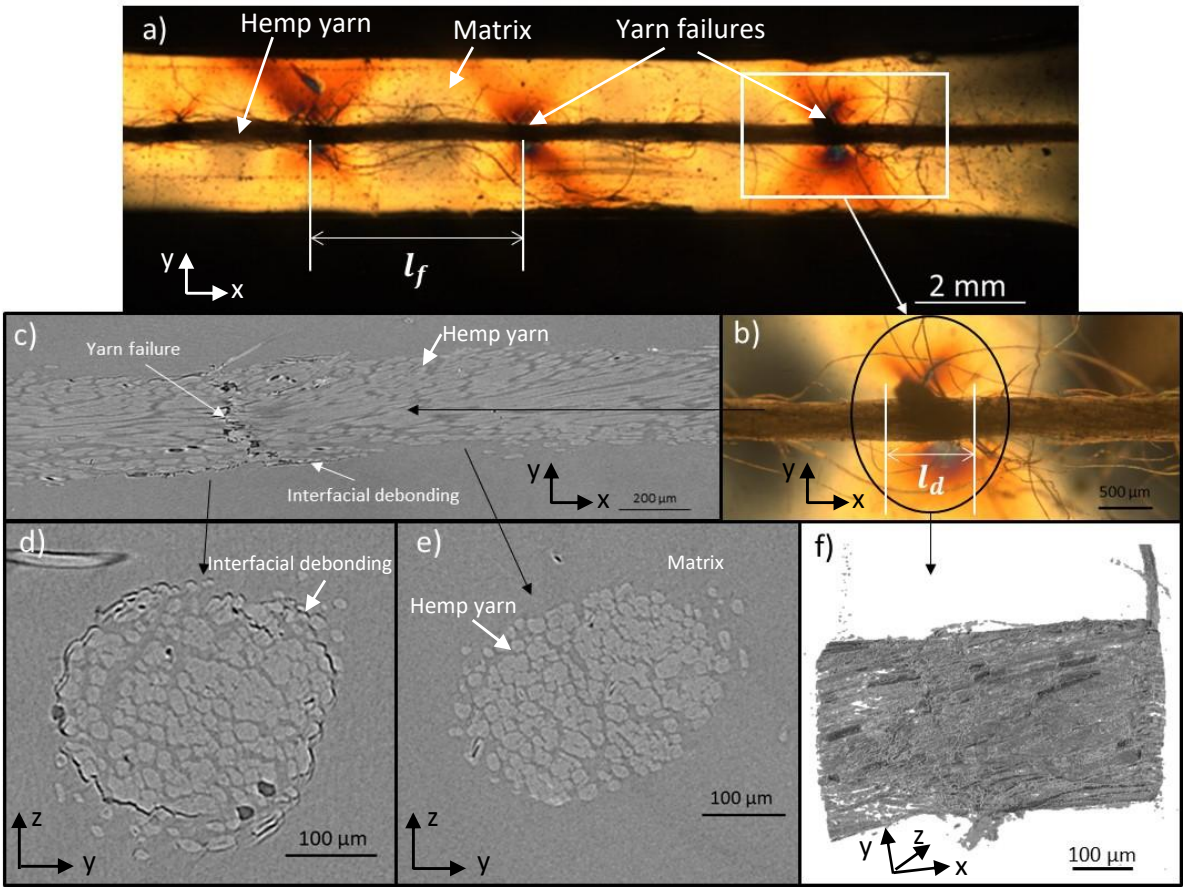

Fig. 11. Microscopic pictures of a single untreated hemp yarn/epoxy composite after fragmentation test. Optical microscope observations with polarised light (a) and focus on one yarn failure (b). Micro-CT observations: longitudinal view of a yarn failure zone (c), cross section in the debonding zone (d), cross section in the healthy zone (e), 3D reconstruction of the damage near the yarn failure zone (f).

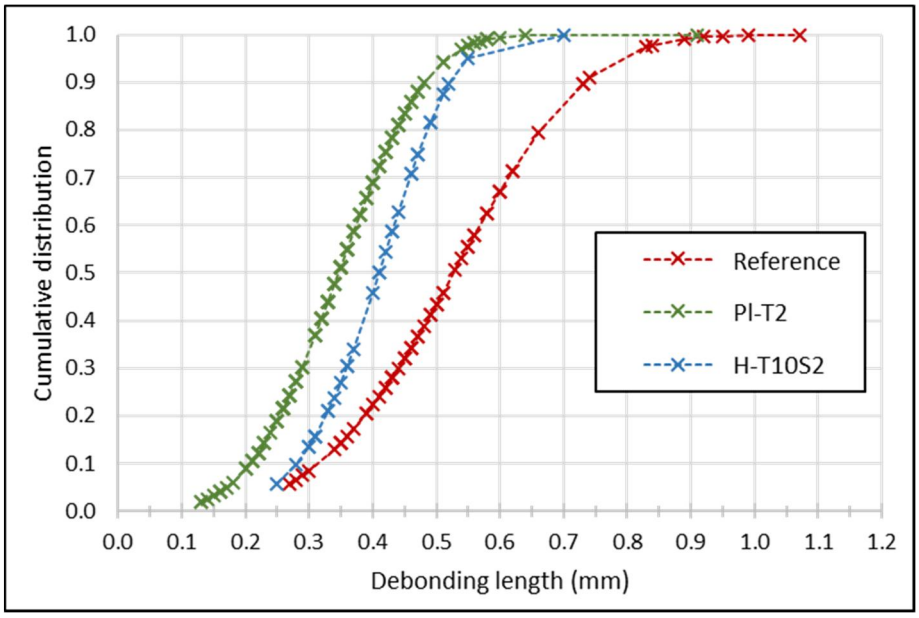

Fig. 12. Cumulative distribution of debonding lengths measured by optical micrography on single hemp yarn/epoxy composites for untreated (reference) and treated hemp yarns: Pl-T2 (Plasma, air 15W) and H-T10S2 (H_2O_2, 10% 103°C).

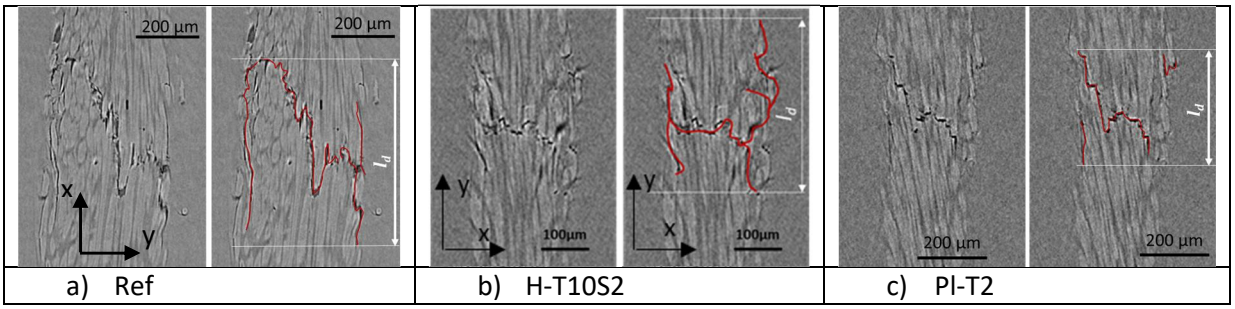

Fig. 13. Micro-CT images of single hemp yarn/epoxy composites after fragmentation tests for a) untreated (reference) hemp yarn and treated hemp yarns: b) H-T10S2 (H_2O_2, 10% 103°C) and c) Pl-T2 (Plasma, air 15W).

Figure captions:

Fig. 1. a) Mould used for sample manufacture. b) Specimen geometry for the single yarn fragmentation tests.

Fig. 2. Scheme of the non-thermal plasma reactor.

Fig. 3. Infrared spectra of the different hemp yarns: untreated (reference) and hydrogen peroxide treated (H-T10S2 and H-T50S2).

Fig. 4. SEM micrographs of hydrogen peroxide treated hemp yarns for three different H_2O_2 concentrations: a) 10%, b) 30% and c) 50%, for the drying sequence S2.

Fig. 5. Infrared spectra after 5 minutes of plasma treatment: A) Pl-T2: air, 15W; B) Pl-T1: air, 25W; C) Pl-T3: O_2, 25W. In each graph, the dark blue spectrum corresponds to the untreated hemp yarn (reference). The other color spectra were taken at four different locations on each treated hemp yarn.

Fig. 6. Tensile strength values of untreated (reference) and hydrogen peroxide treated hemp yarns, for the three H_2O_2 concentrations and the two drying sequences.

Fig. 7. Tensile strength values of untreated (reference) and plasma treated hemp yarns, for the three different configurations: Pl-T1 (air, 25W), Pl-T2 (air, 15W) and Pl-T3 (O_2, 25W).

Fig. 8. Example of fragmentation test on a single hemp yarn/epoxy composite. a) full tensile curve, b) zoom on the tensile curve, c) hemp/epoxy sample with corresponding fragments.

Fig. 9. Cumulative distribution of critical fragment lengths measured on single hemp yarn/epoxy composites for untreated (reference) and treated hemp yarns: Pl-T2 (Plasma, air 15W) and H-T10S2 (H_2O_2, 10% 103°C).

Fig. 10. SEM micrographs of single yarn composite fracture surfaces after fragmentation test. a) for untreated hemp yarn, b) for H_2O_2 treated hemp yarn H-T10S2 (H_2O_2, 10% 103°C) and c) for plasma treated hemp yarn Pl-T2 (Plasma, air 15W).

Fig. 11. Microscopic pictures of a single untreated hemp yarn/epoxy composite after fragmentation test. Optical microscope observations with polarised light (a) and focus on one yarn failure (b). Micro-CT observations: longitudinal view of a yarn failure zone (c), cross section in the debonding zone (d), cross section in the healthy zone (e), 3D reconstruction of the damage near the yarn failure zone (f).

Fig. 12. Cumulative distribution of debonding lengths measured by optical micrography on single hemp yarn/epoxy composites for untreated (reference) and treated hemp yarns: Pl-T2 (Plasma, air 15W) and H-T10S2 (H_2O_2, 10% 103°C).

Fig. 13. Micro-CT images of single hemp yarn/epoxy composites after fragmentation tests for a) untreated (reference) hemp yarn and treated hemp yarns: b) H-T10S2 (H_2O_2, 10% 103°C) and c) Pl-T2 (Plasma, air 15W).